



Article type : Original Article – Platelets

Flavin monooxygenase 3, the host hepatic enzyme in the metaorganismal trimethylamine N-oxide-generating pathway, modulates platelet responsiveness and thrombosis risk

* W. Zhu, * J. A. Buffa, * Z. Wang, * M. Warriar, * R. Schugar, * D. M. Shih, * N. Gupta, † J. C. Gregory, * E. Org, † X. Fu, * L. Li, * J. A. DiDonato, * A. J. Lusic, † J. M. Brown * and S. L. Hazen *
‡ §

*Lerner Research Institute, and ‡Heart and Vascular Institute, Cleveland Clinic, Cleveland, Ohio 44195, USA.

†Departments of Human Genetics and Medicine, David Geffen School of Medicine, University of California, Los Angeles, CA 90095, USA.

§ To whom correspondence should be addressed: Stanley L. Hazen, MD PhD, Department of Cellular & Molecular Medicine, Lerner Research Institute, Cleveland Clinic, 9500 Euclid Avenue, NC-10, Cleveland, OH 44195, Phone: (216) 445-9763, Fax: (216) 444-9404, E-mail: hazens@ccf.org

Short title (running head): Flavin monooxygenase 3 impacts platelet function

Essentials

- Microbe – dependent production of trimethylamine N-oxide (TMAO) contributes to thrombosis risk.
- The impact of host flavin monooxygenase 3 (FMO3) modulation on platelet function is unknown.
- Genetic manipulation of FMO3 in mice alters systemic TMAO levels and thrombosis potential.
- Genetic manipulation of FMO3 is associated with alteration of gut microbial community structure.

This article has been accepted for publication and undergone full peer review but has not been through the copyediting, typesetting, pagination and proofreading process, which may lead to differences between this version and the Version of Record. Please cite this article as doi: 10.1111/jth.14234

This article is protected by copyright. All rights reserved.

Summary.

Background: Gut microbes play a critical role in the production of trimethylamine N-oxide (TMAO), an atherogenic metabolite that impacts platelet responsiveness and thrombosis potential. Involving both microbe and host enzymatic machinery, TMAO generation utilizes a metaorganismal pathway, beginning with ingestion of trimethylamine (TMA)-containing dietary nutrients such as choline, phosphatidylcholine and carnitine, which are abundant in a Western diet. Gut microbial TMA lyases use these nutrients as substrates to produce TMA, which upon delivery to the liver via the portal circulation, is converted into TMAO by host hepatic flavin monooxygenases (FMOs). Gut microbial production of TMA is rate-limiting in the metaorganismal TMAO pathway since hepatic FMO activity is typically in excess.

Objectives: FMO3 is the major FMO responsible for host generation of TMAO; however, a role for FMO3 in altering platelet responsiveness and thrombosis potential *in vivo* has not yet been explored.

Methods: The impact of FMO3 suppression (antisense oligonucleotide-targeting) and overexpression (as transgene), were examined on plasma TMAO levels, platelet responsiveness and thrombosis potential using a murine FeCl₃-induced carotid artery injury model. Cecal microbial composition was examined using 16S analyses.

Results: Modulation of FMO3 directly impacts systemic TMAO levels, platelet responsiveness, and rate of thrombus formation *in vivo*. Microbial composition analyses reveal taxa whose proportions are associated with both plasma TMAO levels and *in vivo* thrombosis potential.

Conclusions: The present studies demonstrate host hepatic FMO3, the terminal step in the metaorganismal TMAO pathway, participates in diet- and gut microbiota-dependent changes in both platelet responsiveness and thrombosis potential *in vivo*.

Key words: cardiovascular disease; choline; gut microbe; blood platelets; thrombosis.

Introduction

Acute thrombotic events represent a leading cause of death and disability in aging populations worldwide[1]. A critical element of thrombosis development is the ability of platelets to become activated, undergo degranulation and clot formation, and promote hemostasis[2]. Importantly, the presence of cardiovascular disease (CVD) and many CVD risk factors are associated with both heightened platelet reactivity and thrombosis risk[3-7]. Despite the contribution of platelet responsiveness to thrombotic event risk[8,9], a clear understanding of the mechanisms that modulate platelet responsiveness and thrombosis susceptibility are not fully defined. Moreover, while anti-platelet agents are a major tool in the current therapeutic arsenal for CVD, their more widespread use is limited by adverse bleeding complications[10,11].

Recent studies show both clinical and mechanistic links between gut microbiota and CVD related phenotypes including atherosclerosis[12-15], adverse ventricular remodeling and heart failure[16-18], and platelet responsiveness and thrombosis potential[19]. Specifically, the gut microbiota-derived metabolite TMAO was shown to contribute to CVD pathogenesis in clinical and basic studies spanning metabolomics, large-scale clinical investigations, microbial transplantation studies and animal models of CVD[12-20]. In studies involving over 4000 subjects, plasma levels of trimethylamine-N-oxide (TMAO) independently predicted incident thrombotic event risk (heart attack and stroke)[19]. Moreover, exposure of human platelets to physiological levels of TMAO altered intracellular calcium signaling, increasing platelet responsiveness to multiple agonists. And dietary choline supplementation was shown to increase plasma TMAO levels, platelet responsiveness, and thrombosis potential in multiple animal models[19]. Importantly, distinct microbial transplantation studies demonstrate TMA/TMAO production capacity with corresponding atherosclerosis and thrombosis potential are all transmissible phenotypes[19,21]. Finally, recent

clinical studies show subjects taking choline supplements have increased plasma TMAO, and heightened platelet responsiveness studies[22].

Production of TMAO occurs via a metaorganismal pathway, relying on the sequential action of both microbial and host enzyme activities. Choline, phosphatidylcholine (lecithin) and carnitine, TMA-containing nutrients abundant in a Western diet, serve as the major dietary precursors for TMAO. When TMA containing nutrients reach the colon, they also serve as nutrients for some microbes, resulting in generation of TMA [12]. TMA produced is transported via the portal circulation to the liver where flavin monooxygenases (FMOs) can catalyze the conversion of TMA into TMAO [23,24]. Of the FMOs, FMO3 serves as the major source of TMA[23], and is the target in the rare genetic disorder trimethylaminuria, also known as “fish odor syndrome”[25,26]. Of note, no CVD or thrombosis related phenotypes are reported with trimethylaminuria. However, FMO3 deficiency leads to low TMAO levels, which is predicted to be associated with reduced risk for thrombosis or atherosclerosis, and thus might be difficult to detect in clinical populations. Antisense oligonucleotide (ASO)-induced FMO3 suppression in mice is reported to reduce TMAO levels and inhibit both atherosclerosis and tissue sterol metabolism[27-29]. The impact of FMO3 activity on platelet function is unknown. Herein we performed genetic manipulation of host FMO3 to determine the impact on TMAO levels, platelet responsiveness and thrombosis potential in vivo.

Methods

General procedures and reagents

Reagents were purchased from Sigma unless otherwise stated. Hepatic FMO activity was quantified using liver homogenate and d9-TMA substrate, monitoring NADPH-dependent production of d9-TMAO[19].

Ethical considerations

All animal model studies were approved by the Institutional Animal Care and Use Committee at the Cleveland Clinic.

Mouse ex vivo platelet aggregometry studies

Platelet-rich plasma (PRP) was generated as described[5]. Diluted platelet-poor plasma was prepared by further centrifugation at 800 x g for 2min. Platelets were counted using a hemocytometer and concentrations adjusted to 2×10^8 /ml with platelet-poor plasma. CaCl_2 and MgCl_2 (both 1mM final) were added immediately before platelet aggregation studies, which were assessed at 37°C using a dual channel Type 500 VS aggregometer (Chrono-log; Havertown, PA) with stirring at 1200rpm.

Flow cytometry

To prepare isolated platelets, 100 nM prostaglandin E1 was added to PRP and then centrifuged at 100 x g (5min, 22°C). The platelet pellet was gently washed with a modified phosphate buffer saline (12mM $\text{Na[PO}_4]$ pH 7.4, 137mM NaCl, 2.7mM KCl, 1mM MgCl_2 and 5.5mM glucose) with 100nM prostaglandin E1, and centrifuged again (500 x g, 5min), and then re-suspended in modified Tyrode's buffer (12mM NaHCO_3 , 0.4mM NaH_2PO_4 , 5mM HEPES, 137mM NaCl, 2.7mM KCl, 5.6mM glucose, 0.35gm% bovine serum albumin, pH 7.4).

P-selectin cell-surface expression was quantified by flow cytometry using FITC-conjugated CD62p antibody (BD Biosciences, Billerica, MA; Cat# 553744; 1/100 dilution, 10min incubation, 22°C). Isotype control antibody (BD Biosciences, Billerica, MA; Cat# 553995) were used in parallel to assess nonspecific binding. Data are presented as median fluorescence intensity (mean+/-SD). Samples were analyzed on an LSRII flow cytometer (BD Biosciences, Billerica, MA) and data analyzed using FlowJo V10 software (Tree Star, Ashland, OR).

Antisense oligonucleotide (ASO)-mediated knock-down of murine FMO3

ASO-mediated knock-down was accomplished using 20-mer phosphorothioate ASOs containing 2'-O-methoxyethyl groups at positions 1-5 and 15-20. Targeted suppression of FMO3 was confirmed by Western analyses of liver homogenates, suppression of liver homogenate FMO activity and plasma TMAO levels. ASOs used in this work were prepared as previously described[30] by IONIS Pharmaceuticals, Inc. (Carlsbad, CA). For initial studies, C57BL/6J mice were injected intraperitoneally twice weekly with 25mg/kg of either non-targeting control ASO (5'-TCCCATTTTCAGGAGACCTGG-3') or ASO directed against murine FMO3 (5'-TGGAAGCATTTCCTTTAAA-3')[29]. For FMO3 ASO studies in Fig. 4, C57BL/6N mice were injected (12.5mg/kg) intraperitoneally twice a week for 6 weeks using either a new non-targeting cET (constrained ethyl chemistry) control ASO (GGCCAATACGCCGTCA) or cET FMO3 ASO (TTTTTTACCGTGCTTT). Unless otherwise indicated, mice were maintained on chemically defined diets supplemented in choline (1.0%). All ASO-targeted loss-of-function experiments were performed in female mice because of the marked suppression of *fmo3* in post-pubertal male mice[23].

Immunoblotting assay

Total protein was quantified using the bicinchoninic acid assay (Bio-Rad, Hercules, CA)[31]. Proteins (50µg) were separated by 4–12% SDS-PAGE, transferred to polyvinylidene difluoride membranes, and detected after incubation with specific antibodies: anti-FMO3 rabbit polyclonal (ABCAM #Ab126790, Cambridge, MA), anti-GAPDH rabbit monoclonal (Cell Signaling Technologies #5174, Danvers, MA), and β-actin (Cell Signaling Technologies #3700, Danvers, MA). ImageJ was used for densitometric analysis.

Liver FMO activity assay, choline TMA lyase activity assay, and mass spectrometry

Total FMO activity in liver homogenate quantified flavin-dependent d9-TMAO production from d9-TMA using tandem mass spectrometry (LC/MS/MS) analyses using d4-choline as internal standard, as described[12]. Stable isotope dilution LC/MS/MS was used to quantify TMA, TMAO and choline in plasma and animal diets, as described[12,32]. Microbial choline TMA lyase activity was quantified by monitoring d9-TMA production from d9-choline substrate using LC/MS/MS analyses[15]. Reactions were stopped by addition of methanolic acidified d4-choline and $^{13}\text{C}_3, ^{15}\text{N}_1$ -TMA internal standard mix, and deproteinated reaction mixtures analyzed on a Shimadzu (Columbia, MD) 8050 triple quadrupole mass spectrometer with UHPLC interface.

Carotid artery thrombosis model

Mice were subjected to common carotid artery FeCl_3 induced injury, and thrombus formation monitored in real-time using intravital fluorescence microscopy and continuous video image capture[19]. Time to cessation of blood flow was determined through inspection of computer images as described[19] by two data analysts blinded to animal group assignments.

Real-Time PCR Analysis

Expression levels of mRNA were calculated based on the $\Delta\Delta$ -CT method. qPCR was conducted using the Applied Biosystems (Beverly, MA) 7500 Real-Time PCR System. Hepatic *fmo3* gene expression, normalized to Cyclophilin A expression, was quantified using the following primers: FMO3 (Fwd: CCCACATGCTTTGAGAGGAG; Rev: GGAAGAGTTGGTGAAGACCG); Cyclophilin A (Fwd: GCGGCAGGTCCATCTACG; Cyclophilin A Rev: GCCATCCAGCCATTGATC)

Whole blood in vitro thrombosis assay.

Microfluidics experiments were performed using the Cellix Microfluidics System (Cellix Ltd., Dublin, Ireland) as described[19]. Where indicated, channels of a Vena8 Fluoro+ biochip were coated with type 1 collagen (150 μ g/ml). Images of the biochip were collected using an HC Plan Apo 20X/0.7NA lens on a Leica DMI6000 inverted microscope equipped with cooled CCD camera. Whole blood from consented healthy volunteers was fluorescently tagged with Calcein AM and pretreated with TMAO (100 μ M, pH 7.4) or normal saline (30min, 22 $^{\circ}$ C) as indicated. Blood was perfused over chips at physiological shear rate (67.5 dynes/cm²) for 3 minutes and fluorescent platelets adhering to the collagen coating were captured every 2 seconds. At the end of the experiment, PBS was drawn through the biochip channels at 2.5 dynes, and ten images were also captured along the length of the channel. Platelet adherence to the chip surface was quantified with computer assisted tomographic analyses[19].

Bleeding time determination

Bleeding time was examined using a tail tip amputation model[33]. Briefly, mice were anesthetized and maintained on a warming pad, and a consistent injury was made 3 mm from the tip of the tail. The tail was immersed in normal saline maintained at 37° C and the cumulative bleeding time was recorded.

Human liver-specific FMO3 transgenic mice

Two different liver-specific human FMO3 transgenic (FMO3-TG) mouse lines were used. Both demonstrated comparable liver FMO3 expression and plasma TMAO levels, and showed comparable phenotypes. For most experiments, the human FMO3-TG mice used were the same as recently described[23]. Briefly, C57BL/6J mice were engineered to contain a liver-specific human FMO3 transgene DNA construct containing 2.2 kb of mouse albumin enhancer/promoter region, the human FMO3 full-length cDNA (1.6 kb) and SV40 intron/polyA sequence (0.9 kb). The transgene DNA construct was microinjected into fertilized eggs of C57BL/6J mice, and the highest FMO3 expressing line was maintained through heterozygous breeding to WT C57BL/6J mice[23]. This original human FMO3-TG mouse line unfortunately was lost. Consequently, a second hepatocyte-specific human FMO3-TG line was generated using full-length human FMO3 cDNA (NM_006894) PCR cloned into the hepatocyte-specific transgenic vector pLiv11 (PMID:19965599) (used only for Fig. 6C). Briefly, ClaI sites were added to 5' and 3' ends, respectively, of human FMO3 cDNA. This cDNA was then cloned into the ClaI restriction site of the pLiv-11 construct. The transgene cassette including human apoE promoter, human FMO3 cDNA, and human apoE hepatic control region was released from the construct by NotI/SpeI digestion. After purification, the transgene was introduced via pro-nuclear microinjection into C57BL/6J mice (Jackson Labs). Transgenic founder lines were established by implanting microinjected embryos into C57BL/6J foster mothers. The transgene cassette was found

to be intact in these lines by PCR screening using a forward primer in the pLiv11 construct (CTTGGTAAATGTGCTGGGATTAG) and a reverse primer in the hFMO3 cDNA (GATGTCCGGAACAAACCATTAC). Mendelian inheritance of the transgene was confirmed by 50% positive offspring from each transgenic founder. For all experiments hemizygous positive FMO3-TG mice (pure C57BL/6J background) were crossed to WT C57BL/6J mice to generate hemizygous liver FMO3-TG mice and WT littermate controls.

Microbiota studies and statistical analyses

Microbial community composition was assessed by sequencing the V4 hypervariable region of the 16S rRNA gene derived from mouse cecum[21]. Microbial DNA was isolated using the MoBio PowerSoil DNA isolation kit per manufacturer's instructions (MoBIO Laboratories, Carlsbad, CA) and sequenced according to previously described methods[34-37] using the Illumina MiSeq platform. For Principal Coordinate Analyses, each sample's sequences were rarefied to 6000 reads to reduce the effect of sequencing depth. To find OTUs that exhibited significant differences between groups the Linear discriminate analysis effect size (LEfSe) analysis was used[38]. A robust Hotelling T2 test was used to examine the difference in the proportion of specific bacterial taxa along with TMAO or occlusion times between treatment groups. False discovery rates (FDRs) of multiple comparisons were estimated for each taxon based on p values resulting from Spearman correlation estimates. All experiments or animal studies were repeated at least 3 times and values are expressed as mean \pm SEM unless otherwise indicated. Kruskal-Wallis test was used for multiple group comparisons of continuous variables and a Chi-square test was used for categorical variables. The Wilcoxon Rank-Sum test was used for two-group comparison. Linear mixed-effect models were used for repeated measure analyses. Spearman-rank correlation for non-normally distributed data was used to analyze associations between quantitative variables. For all other statistical tests $p < 0.05$ was considered significant. Results from all animals in a given experiment were included in analyses using the

indicated number of biological replicates. All data were analyzed using R 3.1.0 (Vienna, Austria) and JMP (SAS Institute).

Results

TMAO enhances murine platelet responsiveness to multiple agonists

Before investigating the role of FMO3 in altering platelet function *in vivo* we examined the effects of TMAO on mouse platelet function. PRP was isolated from mice maintained on a chemically defined diet (Chow: total choline content 0.08gm%; all mouse plasma TMAO levels <5 μ M). The effect of exogenous TMAO (100 μ M versus vehicle) on platelet aggregation stimulated by multiple distinct agonists (ADP and collagen) was examined. Enhanced platelet aggregation response was observed with sub-maximal levels of either ADP (Fig.1A) or collagen (Fig. 1B). Further, using isolated washed murine platelets incubated with TMAO (100 μ M) versus controls (normal saline), surface expression level of platelet P-selectin was significantly ($p<0.008$) increased in response to submaximal stimulation by ADP (1 μ M) in the platelets exposed to TMAO (Figs 1C,D).

*Antisense oligonucleotide (ASO)-mediated knockdown of *fmo3* reduces TMAO, platelet responsiveness to agonists *ex vivo*, and thrombosis potential *in vivo*.*

To determine if the host gene *fmo3* impacts platelet function *in vivo*, we first used ASO-mediated knockdown technology to suppress FMO3 levels in mice maintained on the choline (1gm%) supplemented diet, as described under Methods. FMO3-ASO treatment (versus control) significantly reduced both liver FMO3 protein content ($p=0.007$; Fig. 2A), and total liver FMO activity as monitored by flavin-dependent conversion of d9-TMA into d9-TMAO in liver homogenates ($p=0.0003$; Fig. 2B). While previous studies examining FMO3 ASO treatment of mice on a high-fat,

high-cholesterol diet suggest FMO3 may modulate glucose and lipid metabolism[29], factors known to influence platelet reactivity, in the present studies (not on high-fat/high-cholesterol diet), no effects were observed (Fig. 2C, D). However, as expected, ASO-mediated knock-down of FMO3 did significantly elevate plasma TMA levels, while concurrently also markedly reducing TMAO levels ($p=0.001$ and $p<0.0001$, respectively; Fig. 2E,F). Notably, cecal microbial choline TMA lyase activity measured under anaerobic culture conditions was not significantly impacted by FMO3-ASO treatment (measured as d9-choline \rightarrow d9-TMA, $p=0.10$; Fig. 2G). Collectively, these results confirm FMO3 is a major determinant of systemic host conversion of TMA into TMAO in mice, and demonstrate that the FMO3-targeted ASO probes used both successfully suppressed hepatic FMO3 protein mass and functionally impaired the conversion TMA into TMAO *in vivo*.

To evaluate the impact of FMO3-ASO suppression on platelet function and clot formation *in vivo*, mice were similarly treated (FMO3-targeting versus control ASO) and then PRP was isolated and platelet responsiveness to ADP-dependent stimulation determined using *ex vivo* platelet aggregometry. Compared with control ASO, FMO3-ASO treatment again elicited a 3- to 5-fold reduction in plasma TMAO ($p<0.0001$) and in parallel, reduction in platelet aggregation response was noted to submaximal (1 μ M) ADP stimulation (Fig. 3). A representative platelet aggregometry tracing from each ASO treatment group is shown in Figure 3A, and cumulative analyses and TMAO levels for all mice in each of the ASO treatment groups are shown in Figure 3B. ASO-induced FMO3 suppression resulted in \sim 5-fold reduction in TMAO levels ($p<0.0001$), and in parallel, a significant decrease in platelet aggregation response induced by sub-maximal ADP stimulation ($p<0.001$; Fig. 3B). Thus, reduction in FMO3 via an ASO-based approach both suppressed systemic TMAO levels and reduced platelet responsiveness.

To further examine the physiological impact of suppression of FMO3 in mice we used an *in vivo* carotid artery FeCl₃ injury model of thrombosis (Fig. 3C,D). The overall study design was identical to that used for the *ex vivo* platelet aggregometry studies, with mice on 1gm% choline supplemented diet treated with control versus FMO3-targeted ASO, as indicated. Again, the FMO3-targeted ASO group (relative to control ASO treated) showed significant reduction in TMAO ($p < 0.0001$), and increases in TMA levels ($p < 0.01$). Importantly, the control ASO treated (higher TMAO) group showed both faster rate of growing fluorescent intra-luminal platelet clot, and shorter occlusion time, than the FMO3-targeted ASO group following carotid artery injury ($p < 0.001$; Fig. 3C,D).

Suppression of fmo3 reduces TMAO levels, and platelet adhesion to matrix in whole blood under physiological shear stress, but does not impact tail bleeding time.

In additional studies we examined the impact of FMO3 on platelet adhesion to collagen in whole blood using a microfluidic device under physiological shear forces (Fig. 4). For these studies we used a distinct murine FMO3-targeting ASO sequence, as described under Methods. Control studies with both mRNA, Western blot analyses (Fig. 4A) and functional measures of plasma TMA and TMAO levels (Fig. 4A) and liver total FMO activity (Fig. 4B) all confirmed suppression (all $P < 0.001$) of host hepatic FMO3 with the FMO3-targeting ASO. Moreover, FMO3 suppression significantly decreased collagen-dependent platelet adhesion to matrix in whole blood under physiological shear force (Fig. 4C). In additional studies, mice similarly treated with the FMO3-targeted versus control ASO were examined for tail bleeding time. Despite significant reduction in systemic TMAO levels in the FMO3-ASO group ($p < 0.001$ versus control ASO), no differences were observed in bleeding time ($p = 0.49$; Fig. 4D).

Liver-specific expression of the human FMO3 transgene enhances systemic TMAO levels, platelet responsiveness to agonists ex vivo, and thrombosis potential in vivo.

We next sought to test the converse hypotheses, namely, that higher levels of FMO3 in mice can result in higher TMAO levels and enhanced susceptibility to thrombosis. We recently described construction of a liver-specific human FMO3-TG mouse[23] and used these for our initial studies. Because FMO3 expression shows considerable sexual dimorphism in mice and is already highly expressed in liver of adult females, but much lower in adult males[12,23], we were concerned that introduction of the human FMO3 transgene might not further increase TMAO levels compared to WT female mice (i.e. if FMO3 is already in excess in females). Indeed, in initial studies we observed that TMAO levels were similar in WT versus FMO3-TG mice regardless of diet (i.e. plasma TMAO from WT v FMO3-TG mice on chow diet, $p=0.97$; on choline supplemented diet, $p=0.37$, data not shown). In contrast, parallel studies in male mice showed significant increase in circulating TMAO with the introduction of the human FMO3 transgene ($n>5$ each genotype, $p<0.01$; see below). We therefore performed all FMO3 gain-of-function studies in male mice (WT versus their heterozygote littermates for the human *fmo3* transgene).

Results of initial characterization studies of the male FMO3-TG mice are shown in Figure 5. Mice were maintained on the choline supplemented (1gm%) diets from time of weaning, as described under Methods. As shown, FMO3-TG mice (versus WT) had higher levels of both hepatic FMO3 mRNA and protein ($p<0.05$, each; Figure 5A). Functional analyses confirmed the FMO3-TG mice had higher liver FMO activity (measured as flavin dependent conversion of d9-TMA \rightarrow d9-TMAO) than their WT littermates ($p=0.006$; Figure 5B). No significant change in plasma glucose or cholesterol levels were noted (Figure 5C, 5D), but as anticipated, higher TMAO levels were observed ($p=0.0005$; Fig. 5F). Surprisingly, plasma TMA levels in the FMO3-TG mice were also significantly higher than that in WT littermates ($p=0.01$; Fig. 5E), suggesting enhanced microbial production; however, direct

Accepted Article
measurement of cecal microbial choline TMA lyase activity during anaerobic culture showed no differences between FMO3-TG mice and their WT littermates ($p=0.3$; Fig. 5G).

Since plasma TMAO levels were increased in the male FMO3-TG animals, we proceeded to evaluate the impact of FMO3 transgene on platelet function and thrombosis potential. The higher TMAO levels observed ($p<0.001$) in FMO3-TG mice were accompanied by heightened platelet responsiveness to ADP as monitored by platelet aggregometry (Fig. 6A,B; $p<0.001$). To determine whether there is any indication of platelet priming in mice induced solely by FMO3 overexpression, isolated washed platelets from the FMO3-TG versus WT mice (on chow diet) were examined by flow cytometry for P-selectin surface expression, as described under Methods. No changes in P-selectin levels were noted between the groups ($p=0.67$; Fig. 6C).

In further studies we sought to examine the functional impact of FMO3 overexpression on susceptibility for thrombosis *in vivo*. Animals were maintained on a choline supplemented diet and rates of thrombus formation and time to vessel occlusion monitored in the carotid artery following FeCl_3 - induced injury. Notably, the FMO3-TG mice showed higher TMAO levels, which was accompanied by faster clot formation and significantly shorter time to vessel occlusion ($p<0.001$; Fig. 6D,E). In additional analyses we pooled data from all animal studies (both ASO silencing and FMO3 overexpression) and observed a significant relationship between plasma TMAO levels and platelet responsiveness ($R=0.44$ (Spearman), $p=0.01$; Figure 7A).

Genetic manipulation of FMO3 is associated with alteration of gut microbial community

In a final series of studies, because of the observed elevation in TMA in FMO3-TG mice above, and the recent observation that alteration in FMO3 can impact bile acid pool size and composition[29], which can impact microbial community structure, we decided to examine whether hepatic human FMO3 overexpression impacted microbial composition in the mice. Cecal microbial DNA was recovered from mice used in *in vivo* thrombosis model studies, and the DNA encoding 16S ribosomal RNA was analyzed. Significant differences in community structure were observed between microbes recovered from FMO3-TG versus WT mice as visualized using Principal Coordinates Analysis (Fig. 7B, $p < 0.001$ for Student's t test with 1,000 Monte Carlo simulations). Subsequent examination of the microbial communities using Linear Discriminant Analysis coupled with effect size measurements (LEfSe)[19] identified three cecal microbial taxa whose proportions were characteristic of the FMO3-TG mice (versus WT littermates), and 1 taxa characteristic of WT mice (Fig. 7C). In further analyses (Figure 7D-G) the proportions of three taxa (*Desulfovibrionaceae*, *Lactobacillus* and *Dehalobacterium*) recovered from cecum of FMO3-TG mice were both significantly positively associated with TMAO levels, and negatively associated with occlusion time - the same 3 taxa identified as being characteristic of FMO3-TG mice through LEfSe analyses (Fig. 7C). Further, the proportions of the genus *Odoribacter*, which was identified as being characteristic of WT (versus FMO3 heterozygotes; Fig. 7C), was also observed to be both significantly negatively associated with TMAO and positively associated with *in vivo* time to occlusive clot formation (Fig. 7G). In further analyses among all mice (both FMO3-TG and WT controls), 3 taxa were identified whose proportions were significantly associated with quantitative measures of thrombosis potential (occlusion time) *in vivo* (family *Prevotellaceae*, genus *Prevotella*, and genus *Desulfovibrionaceae*, all FDR adjusted $p \leq 0.01$; Fig. 7H).

Discussion

Normal platelet function is critical to maintain blood hemostasis in a closed circulatory system. And yet, increased platelet responsiveness is associated with elevated CVD risks and heightened rate of thrombotic events. Platelet hyperresponsiveness and thrombosis risk are associated with numerous conditions that predispose to CVD such as hyperlipidemia[3], oxidative stress[4] and hyperglycemia[5]. Yet the underlying mechanism(s) remain incompletely understood. We recently showed that the microbe-dependent metabolite, TMAO, directly modulates platelet responsiveness via alteration in calcium release from intracellular pools[19]. Parallel animal model studies showed direct infusion and acute elevation of circulating TMAO can enhance *in vivo* thrombosis potential in multiple animal models[19]. More recent interventional studies in humans show choline supplementation raises TMAO levels in healthy volunteers (both omnivores and vegans alike) and enhances platelet responsiveness[22]. Moreover, large scale clinical association studies (e.g. n>4000 subjects) independently demonstrate that plasma TMAO levels are associated with incident risk of thrombotic events[19]. Interestingly, the heightened thrombosis potential observed with TMAO elevation *in vivo* may arise not only from alterations in platelet responsiveness, but also alternative mechanisms operative at the artery wall (Figure 7). For example, Seldin and colleagues recently reported that direct injection of TMAO *in vivo* results in vascular inflammation, including arterial endothelial cell activation and up-regulation of adhesion proteins through signaling via Mitogen-Activated Protein Kinase and NFkB[39].

The metaorganismal pathway responsible for TMAO generation involves both the initiating microbial production of TMA, and the host conversion of TMA into TMAO. In the present studies we utilize multiple independent and complementary approaches to investigate the second half of the TMAO metaorganismal pathway, host FMO3. Using both genetic silencing and gain of function approaches, our studies unambiguously show the involvement of FMO3, via its participation in TMAO generation,

Accepted Article
as a regulator of both platelet responsiveness, and *in vivo* thrombosis potential. It has been suggested that we are holobionts (i.e. assemblages of both host and all of its symbiotic microbes), and to optimally understand physiology, one needs to understand the totality of metabolic processes mediated by both host and microbes within[40]. The present studies build on this concept, and further define a nutrient → microbe → host metaorganismal pathway that produces TMAO and consequently, alters platelet function and thrombosis potential *in vivo* (Fig. 8).

Anti-platelet therapies are a cornerstone for cardiovascular risk reduction in modern medicine[41,42]. Moreover, the intra-coronary arterial sites of culprit lesions in subjects with acute myocardial infarction typically have less than 50% stenosis[e.g. reviewed in 43], and it is the acute thrombotic event that precipitates a myocardial infarction, stroke or often sudden cardiac death[44]. Despite their many benefits, anti-platelet agents, including low dose aspirin, are limited by their tendency to foster unwanted bleeding events[45-47]. Thus there is compelling need to optimize CVD event reduction without accompanying untoward bleeding complications. The present studies suggest targeting the TMAO metaorganismal pathway may be a rational approach. Notably, individuals with a genetic defect in FMO3 have not been reported to have accompanying bleeding complications. Moreover, with FMO3 suppression via ASO, reduced TMAO and both reduced platelet responsiveness and thrombosis potential were observed. Of note, there was no evidence of prolongation in the occlusion time during *in vivo* thrombosis studies with FMO3 ASO treatment. While the present studies provide confirmatory support for involvement of this metaorganismal pathway in thrombosis potential, FMO3 remains a poor pharmacological target given the resultant TMA elevation and fish odor that accompanies successful suppression of FMO3 activity. Beyond converting TMA to TMAO, FMOs are also known primarily for their role in metabolism of a wide variety of drugs and environmental pollutants[48-50]. Thus, pharmacological inhibition of FMO3,

although it would potentially reduce host TMAO generation and not impact normal platelet function, would also be predicted to interrupt a central host drug metabolism and detoxification route.

In summary, the present studies further reveal involvement of a gut microbiota-dependent pathway that impacts host vascular function via effects on hemostasis and clot formation. They reaffirm a mechanistic link between dietary choline, a nutrient abundant in a Western diet, gut microbes, and host hepatic conversion of the gut microbial intermediate TMA into TMAO, an end product that both impacts platelet function and enhances thrombosis susceptibility. Further studies targeting the TMAO metaorganismal pathway for the treatment of atherothrombotic disease are warranted.

Addendum

W. Zhu participated in the design, performance and analyses of most studies and the drafting of the manuscript. J. A. Buffa, M. Warriar, R. Schugar, D. M. Shih, J. C. Gregory and N. Gupta participated in the gain of function and loss of function animal model studies. Z. Wang, M. and X. Fu performed mass spectrometry analyses. L. Li assisted with statistical analyses. E. Org and A. J. Lusic performed gut microbial composition analyses. J. A. DiDonato and J. M. Brown assisted with experimental design, input and thoughtful discussions. S. L. Hazen conceived of the project idea, and participated in the design of experiments, data analyses and the drafting of the manuscript. All authors critically reviewed and edited the manuscript.

Acknowledgements

ASO probes employed were generously provided by Ionis Pharmaceuticals. This research was supported by grants from the National Institutes of Health and the Office of Dietary Supplements

(HL103866, HL126827 and DK106000 (to S.L. Hazen), 2P01HL030568-31A1, HL28481 and HL30568 (to A.J. Lusis), HL130819 (to Z. Wang) and HL122283 (to J.M. Brown)). W. Zhu was supported in part by an American Heart Association Scientist Development Grant. E. Org was supported in part by FP7 grant no 330381.

Disclosure of Conflict of Interest

S.L. Hazen and Z. Wang are named as co-inventors on pending and issued patents held by the Cleveland Clinic relating to cardiovascular diagnostics or therapeutics. S.L. Hazen and Z. Wang report having the right to receive royalty payment for inventions or discoveries related to cardiovascular diagnostics from Cleveland Heart Lab, Inc. S.L. Hazen also reports having been paid as a consultant for P&G, and receiving research funds from Astra Zeneca, P&G, Pfizer Inc., and Roche Diagnostics.

The other authors state that they have no conflict of interest.

References

1. Roth GA, Forouzanfar MH, Moran AE, Barber R, Nguyen G, Feigin VL, Naghavi M, Mensah GA, Murray CJ. Demographic and epidemiologic drivers of global cardiovascular mortality. *N Engl J Med* 2015; **372**: 1333-41.
2. Jackson SP, Nesbitt WS, Westein E. Dynamics of platelet thrombus formation. *J Thromb Haemost* 2009; **7**: 17-20.
3. Podrez EA, Byzova TV, Febbraio M, Salomon RG, Ma Y, Valiyaveettil M, Poliakov E, Sun M, Finton PJ, Curtis BR, Chen J, Zhang R, Silverstein RL, Hazen SL. Platelet CD36 links hyperlipidemia, oxidant stress and a prothrombotic phenotype. *Nat Med* 2007; **13**: 1086-95.
4. Chen K, Febbraio M, Li W, Silverstein RL. A specific CD36-dependent signaling pathway is required for platelet activation by oxidized low-density lipoprotein. *Circ Res* 2008; **102**: 1512-19.

- Accepted Article
5. Zhu W, Li W, Silverstein RL. Advanced glycation end products induce a prothrombotic phenotype in mice via interaction with platelet CD36. *Blood* 2012; **119**: 6136-44.
 6. Rollini F, Franchi F, Muñoz-Lozano A, Angiolillo DJ. Platelet function profiles in patients with diabetes mellitus. *J Cardiovasc Transl Res* 2013; **6**: 329-45.
 7. Marcucci R, Valente S, Gori AM, Chiostrì M, Panicia R, Giusti B, Cau V, Lazzeri C, Gensini GF, Abbate R. Global platelet hyperreactivity and elevated C-reactive protein levels predict long term mortality in STEMI patients. *Thromb Res* 2014; **134**: 884-88.
 8. Frossard M, Fuchs I, Leitner JM, Hsieh K, Vlcek M, Losert H, Domanovits H, Schreiber W, Laggner AN, Jilma B. Platelet function predicts myocardial damage in patients with acute myocardial infarction. *Circulation* 2004; **110**: 1392-97.
 9. Tantry US, Bonello L, Aradi D, Price MJ, Jeong YH, Angiolillo DJ, Stone GW, Curzen N, Geisler T, Ten Berg J, Kirtane A, Siller-Matula J, Mahla E, Becker RC, Bhatt DL, Waksman R, Rao SV, Alexopoulos D, Marcucci R, Reny JL, et al. Working Group on On-Treatment Platelet Reactivity. Consensus and update on the definition of on-treatment platelet reactivity to adenosine diphosphate associated with ischemia and bleeding. *J Am Coll Cardiol* 2013; **62**: 2261-73.
 10. Jennings LK. Mechanisms of platelet activation: need for new strategies to protect against platelet-mediated atherothrombosis. *Throm. Haemost* 2009; **102**: 248-57.
 11. Becker RC, Gibson CM, Jennings LK, Morrow DA. Antiplatelet therapy in acute coronary syndrome (ACS): applying new science to clinical decisions. *Am J Cardiol* 2010; **106**: S2-S3.
 12. Wang Z, Klipfell E, Bennett BJ, Koeth R, Levison BS, Dugar B, Feldstein AE, Britt EB, Fu X, Chung YM, Wu Y, Schauer P, Smith JD, Allayee H, Tang WH, DiDonato JA, Lusis AJ, Hazen SL. Gut flora metabolism of phosphatidylcholine promotes cardiovascular disease. *Nature* 2011; **472**: 57-63.
 13. Koeth RA, Wang Z, Levison BS, Buffa JA, Org E, Sheehy BT, Britt EB, Fu X, Wu Y, Li L, Smith JD, DiDonato JA, Chen J, Li H, Wu GD, Lewis JD, Warrier M, Brown JM, Krauss RM, Tang WH, et al. Intestinal microbiota metabolism of L-carnitine, a nutrient in red meat, promotes atherosclerosis. *Nat Med* 2013; **19**: 576-85.
 14. Tang WH, Wang Z, Levison BS, Koeth RA, Britt EB, Fu X, Wu Y, Hazen SL. Intestinal microbial metabolism of phosphatidylcholine and cardiovascular risk. *N Engl J Med* 2013; **368**: 1575-84.
 15. Koeth RA, Levison BS, Culley MK, Buffa JA, Wang Z, Gregory JC, Org E, Wu Y, Li L, Smith JD, Tang WH, DiDonato JA, Lusis AJ, Hazen SL. γ -Butyrobetaine is a proatherogenic intermediate in gut microbial metabolism of L-carnitine to TMAO. *Cell Metab* 2014; **20**: 799-812.
 16. Tang WH, Wang Z, Fan Y, Levison B, Hazen JE, Donahue LM, Wu Y, Hazen SL. Prognostic value of elevated levels of intestinal microbe-generated metabolite trimethylamine-N-oxide in patients with heart failure: refining the gut hypothesis. *J Am Coll Cardiol* 2014; **64**: 1908-14.

- Accepted Article
17. Organ CL, Otsuka H, Bhushan S, Wang Z, Bradley J, Trivedi R, Polhemus DJ, Tang WH, Wu Y, Hazen SL, Lefer DJ. Choline Diet and Its Gut Microbe-Derived Metabolite, Trimethylamine N-Oxide, Exacerbate Pressure Overload-Induced Heart Failure. *Circ Heart Fail* 2016; **9**: e002314
 18. Trøseid M, Ueland T, Hov JR, Svoldal A, Gregersen I, Dahl CP, Aakhus S, Gude E, Bjørndal B, Halvorsen B, Karlsen TH, Aukrust P, Gullestad L, Berge RK, Yndestad A. Microbiota-dependent metabolite trimethylamine-N-oxide is associated with disease severity and survival of patients with chronic heart failure. *J Intern Med* 2015; **277**: 717-26.
 19. Zhu W, Gregory JC, Org E, Buffa JA, Gupta N, Wang Z, Li L, Fu X, Wu Y, Mehrabian M, Sartor RB, McIntyre TM, Silverstein RL, Tang WH, DiDonato JA, Brown JM, Lusic AJ, Hazen SL. Gut Microbial Metabolite TMAO Enhances Platelet Hyperreactivity and Thrombosis Risk. *Cell* 2016; **165**: 111-24.
 20. Li XS, Obeid S, Klingenberg R, Gencer B, Mach F, Räber L, Windecker S, Rodondi N, Nanchen D, Muller O, Miranda MX, Matter CM, Wu Y, Li L, Wang Z, Alamri HS, Gogonea V, Chung YM, Tang WH, Hazen SL, et al. Gut microbiota-dependent trimethylamine N-oxide in acute coronary syndromes: a prognostic marker for incident cardiovascular events beyond traditional risk factors. *Eur Heart J* 2017; **38**: 814-24.
 21. Gregory JC, Buffa JA, Org E, Wang Z, Levison BS, Zhu W, Wagner MA, Bennett BJ, Li L, DiDonato JA, Lusic AJ, Hazen SL. Transmission of atherosclerosis susceptibility with gut microbial transplantation. *J Biol Chem* 2015; **290**: 5647-60.
 22. Zhu W, Wang Z, Tang WH, Hazen SL. Gut microbe-generated Trimethylamine N-Oxide from dietary choline is prothrombotic in subjects. *Circulation* 2017; **135**: 1671-73.
 23. Bennett BJ, de Aguiar Vallim TQ, Wang Z, Shih DM, Meng Y, Gregory J, Allayee H, Lee R, Graham M, Crooke R, Edwards PA, Hazen SL, Lusic AJ. Trimethylamine-N-oxide, a metabolite associated with atherosclerosis, exhibits complex genetic and dietary regulation. *Cell Metab* 2013; **17**: 49-60.
 24. Schugar RC, Brown JM. Emerging roles of flavin monooxygenase 3 in cholesterol metabolism and atherosclerosis. *Curr Opin Lipidol* 2015; **26**: 426-31.
 25. Dolphin CT, Janmohamed A, Smith RL, Shephard EA, Phillips IR. Missense mutation in flavin-containing mono-oxygenase 3 gene, FMO3, underlies fish-odour syndrome. *Nat Genet* 1997; **17**: 491-94.
 26. Khan SA, Shagufta K. A rare case of fish odor syndrome presenting as depression. *Indian J Psychiatry* 2014; **56**: 185-87.
 27. Miao J, Ling AV, Manthena PV, Gearing ME, Graham MJ, Crooke RM, Croce KJ, Esquejo RM, Clish CB, Group. MOS, Vicent D, Biddinger SB. Flavin-containing monooxygenase 3 as a potential player in diabetes-associated atherosclerosis. *Nat Commun* 2015; **6**: 6498
 28. Shih DM, Wang Z, Lee R, Meng Y, Che N, Charugundla S, Qi H, Wu J, Pan C, Brown JM, Vallim T, Bennett BJ, Graham M, Hazen SL, Lusic AJ. Flavin containing monooxygenase 3 exerts

broad effects on glucose and lipid metabolism and atherosclerosis. *J. Lipid Res* 2015; **56**: 22-37.

29. Warriar M, Shih DM, Burrows AC, Ferguson D, Gromovsky AD, Brown AL, Marshall S, McDaniel A, Schugar RC, Wang Z, Sacks J, Rong X, Vallim TA, Chou J, Ivanova PT, Myers DS, Brown HA, Lee RG, Crooke RM, Graham MJ, et al. The TMAO-Generating Enzyme Flavin Monooxygenase 3 Is a Central Regulator of Cholesterol Balance. *Cell Rep* 2015; **10**: 326-38.
30. Crooke RM, Graham MJ, Lemonidis KM, Whipple CP, Koo S, Perera RJ. An apolipoprotein B antisense oligonucleotide lowers LDL cholesterol in hyperlipidemic mice without causing hepatic steatosis. *J Lipid Res* 2005; **46**: 872-84.
31. Brown JM, Boysen MS, Chung S, Fabiyi O, Morrison RF, Mandrup S, McIntosh MK. Conjugated linoleic acid induces human adipocyte delipidation: autocrine/paracrine regulation of MEK/ERK signaling by adipocytokines. *J Biol Chem* 2004; **279**: 26735-47.
32. Wang Z, Levison BS, Hazen JE, Donahue L, Li XM, Hazen SL. Measurement of trimethylamine-N-oxide by stable isotope dilution liquid chromatography tandem mass spectrometry. *Anal Biochem* 2014; **455**: 35-40.
33. Liu Y, Jennings NL, Dart A M, Du XJ. Standardizing a simpler, more sensitive and accurate tail bleeding assay in mice. *World J. Exp. Med.* 2012; **2**, 30–36.
34. Caporaso JG, Lauber CL, Walters WA, Berg-Lyons D, Huntley J, Fierer N, Owens SM, Betley J, Fraser L, Bauer M, Gormley N, Gilbert JA, Smith G, Knight R. Ultra-high-throughput microbial community analysis on the Illumina HiSeq and MiSeq platforms. *ISME J* 2012; **6**: 1621-24.
35. Bokulich NA, Subramanian S, Faith JJ, Gevers D, Gordon JI, Knight R, Mills DA, Caporaso JG. Quality-filtering vastly improves diversity estimates from Illumina amplicon sequencing. *Nat Methods* 2013; **10**: 57-59
36. Edgar RC. Search and clustering orders of magnitude faster than BLAST. *Bioinformatics* 2010; **26**: 2460-61.
37. McDonald D, Price MN, Goodrich J, Nawrocki EP, DeSantis TZ, Probst A, Andersen GL, Knight R, Hugenholtz P. An improved Greengenes taxonomy with explicit ranks for ecological and evolutionary analyses of bacteria and archaea. *ISME J* 2012; **6**: 610-18.
38. Segata N, Waldron L, Ballarini A, Narasimhan V, Jousson O, Huttenhower C. Metagenomic microbial community profiling using unique clade-specific marker genes. *Nat Methods* 2012; **9**: 811-14.
39. Seldin MM, Meng Y, Qi H, Zhu W, Wang Z, Hazen SL, Lusis AJ, Shih DM. Trimethylamine N-Oxide Promotes Vascular Inflammation Through Signaling of Mitogen-Activated Protein Kinase and Nuclear Factor- κ B. *J Am Heart Assoc.* 2016; **5**(2).
40. Margulis L. Symbiosis as a Source of Evolutionary Innovation: Speciation and Morphogenesis. *Chapter 1: Symbiogenesis and Symbioticism, by Lynn Margulis. 1-14. MIT Press. Cambridge MA*

- Accepted Article
41. Wright RS, Anderson JL, Adams CD, Bridges CR., Casey DE Jr., Ettinger SM, Fesmire FM, Ganiats TG, Jneid H, Lincoff AM, Peterson ED, Philippides GJ, Theroux P, Wenger NK, Zidar JP, Jacobs AK. ACCF/AHA Focused Update of the Guidelines for the Management of Patients With Unstable Angina/ Non-ST-Elevation Myocardial Infarction (Updating the 2007 Guideline): a report of the American College of Cardiology Foundation/American Heart Association Task Force on Practice Guidelines. *Circulation* 2011; **123**: 2022-260.
 42. Cerbone AM, Macarone-Palmieri N, Saldalamacchia G, Coppola A, Di Minno G, Rivellese AA. Diabetes, vascular complications and antiplatelet therapy: open problems. *Acta Diabetol* 2009; **46**: 253-61.
 43. Arbab-Zadeh A, Nakano M, Virmani R, Fuster V. Acute coronary events. *Circulation* 2012; **125**: 1147-56.
 44. Hayashi M, Shimizu W, Albert CM. The spectrum of epidemiology underlying sudden cardiac death. *Circ Res* 2015; **116**: 1887-906.
 45. Gillette M, Morneau K, Hoang V, Virani S, Jneid H. Antiplatelet Management for Coronary Heart Disease: Advances and Challenges. *Curr. Atheroscler Rep* 2016; **18**: 35.
 46. Bittl JA, Baber U, Bradley SM, Wijeyesundera DN. Duration of Dual Antiplatelet Therapy: A Systematic Review for the 2016 ACC/AHA Guideline Focused Update on Duration of Dual Antiplatelet Therapy in Patients With Coronary Artery Disease: A Report of the American College of Cardiology/American Heart Association Task Force on Clinical Practice Guidelines. *J Am Coll Cardiol* 2016; **68**: 1116-39.
 47. Gurbel PA, Jeong YH, Navarese EP, Tantry US. Platelet-Mediated Thrombosis: From Bench to Bedside. *Circ Res* 2016; **118**: 1380-91.
 48. Lin J, Cashman JR. Detoxication of tyramine by the flavin-containing monooxygenase: stereoselective formation of the trans oxime. *Chem Res Toxicol* 1997; **8**: 842-52.
 49. Krueger SK, Williams DE. Mammalian flavin-containing monooxygenases: structure/function, genetic polymorphisms and role in drug metabolism. *Pharmacol Ther* 2005; **106**: 357-87.
 50. Fennema D, Phillips IR, Shephard EA. Trimethylamine and Trimethylamine N-Oxide, a Flavin-Containing Monooxygenase 3 (FMO3)-Mediated Host-Microbiome Metabolic Axis Implicated in Health and Disease. *Drug Metab Dispos* 2016; **44**: 1839-50.

Figure legends:

Figure 1. Brief exposure of platelets to TMAO enhances platelet responsiveness. (A-B) Platelet rich plasma (PRP) was recovered from C57BL/6J female mice (maintained on chow diet) and then incubated in the presence of TMAO (100 μ M) versus vehicle (normal saline, “-TMAO”) control for 15 min as described under Methods. Platelet aggregometry response following stimulation with the indicated concentrations of either ADP (A) or collagen (B) were then examined. Data represent the % of maximum aggregometry amplitude (mean \pm SD) from the indicated number of distinct biological replicates (mice). (C-D) Platelets were isolated from C57BL/6J female mice maintained on chow diet, washed, and then incubated with either TMAO (100 μ M) or vehicle (normal saline) as described under Methods. At time of exposure to ADP (1 μ M), either anti P-selectin or isotype control antibody were concurrently added, and then following 10min, cells were fixed and surface expression of P-selectin was quantified by flow cytometry, as described under Methods . Illustrative flow cytometry tracings (C) and quantitative P-selectin surface expression (median fluorescence intensity, \pm SD) from the indicated number of mice (D) are shown. P values shown were calculated using Kruskal-Wallis test(A,B) and Wilson rank-sum test was used for two-group comparison (D).

Figure 2. Antisense oligonucleotide (ASO)-mediated knockdown of *fmo3* reduces plasma TMAO levels without altering cecal microbial choline TMA lyase activity. (A-E) C57BL/6J mice maintained on a choline supplemented (1%) diet were injected intraperitoneally with either a murine FMO3-targeting ASO or control ASO for 6 weeks as described under Methods. (A) Quantitative immunoblot results for liver FMO3 protein (normalized by GAPDH) are shown (as mean \pm SEM), along with Western Blot images. (B) Liver total FMO activity was measured in both groups. The middle line represents mean and whiskers represent SEM. Plasma levels of (C) glucose, (D) total cholesterol, (E) TMA, (F) TMAO and (G) cecal choline TMA lyase enzyme activity, were quantified as described in

Methods. For each, the middle line represents mean and whiskers represent SD for the indicated numbers of mice. The Wilson rank-sum test was used for two-group comparison.

Figure 3. ASO-mediated suppression of liver *fmo3* reduces TMAO-induced platelet responsiveness *ex vivo*, and *in vivo* thrombosis potential as monitored using the carotid artery FeCl₃-induced injury model. (A-D) C57BL/6J mice maintained on a choline supplemented diet were injected intraperitoneally with either a murine FMO3-targeting ASO or control ASO for 6 weeks, as described under Methods. (A, B) Platelet rich plasma was recovered, and aggregometry responses were monitored following stimulation with sub-maximal (1 μ M final) ADP. (A) Representative aggregation tracing in response to 1 μ M ADP from a mouse within each group, along with the TMA and TMAO level in the mouse at time of study. (B) Cumulative data from mice in each group. Data represent the % of max aggregometry amplitude in response to 1 μ M ADP, along with mean (\pm SEM) plasma TMA and TMAO levels, for each of the mouse groups. (C, D) Time to cessation of flow was quantified following FeCl₃-induced carotid artery injury, along with plasma TMA and TMAO levels, as described under Methods. In all panels, the middle line represents mean and whiskers represent SEM. (D) Shown are representative vital microscopy images of carotid artery thrombus formation at the indicated time points following arterial injury. The Wilcoxon Rank-Sum test was used for two-group comparison.

Figure 4. ASO-mediated suppression of liver *fmo3* reduces platelet adhesion and spreading to immobilized collagen matrix in whole blood under physiological shear stress, but does not impact tail bleeding time.

(A-D) C57BL/6N mice were injected intraperitoneally with either a murine FMO3-targeting ASO or control ASO for 6 weeks as described under Methods. One week prior to study, mice were placed on

a 0.5% choline supplemented diet. On day of study, (A) liver FMO3 mRNA and plasma TMA and TMAO, liver FMO3 protein by Western analysis (n=4 each group, normalized by Actin), and (B) liver total FMO activity were quantified as described under Methods. Data reported are mean \pm SEM (middle line and whiskers) for the indicated numbers of mice. (C) Platelet adhesion in whole blood to a microfluidic chip surface (\pm collagen coating) was quantified under physiological shear as described under Methods. Data represents mean \pm SEM adherent platelet area per unit area (μ^2) of chip surface. Representative images of platelet adhesion from each group at end point following fixation is shown in the images to the right. (D) Tail bleeding time were measured as described in Methods. Data represents mean \pm SD (middle line and whiskers) for the indicated numbers of mice. The Wilcoxon Rank-Sum test was used for two-group comparison.

Figure 5. Characterization of mice with over expression of human *fmo3* transgene. Human FMO3-TG mice and their WT littermates were maintained on a choline-supplemented (1%) diet for 6 weeks as described under Methods. On day of study, mice were sacrificed and (A) Liver FMO3 mRNA (house-keeping gene for normalization was TBP) and protein levels (normalized by Actin) were evaluated. Shown are mean (\pm SEM) and Western Blot images. (B) Liver total FMO activity was quantified in liver homogenates by monitoring the conversion of d9-TMA into d9-TMAO, as described under Methods. Plasma levels of (C) glucose, (D) cholesterol, (E) TMA and (F) TMAO were also quantified as described under Methods. (G) Cecal choline TMA lyase activity was quantified by monitoring the conversion of d9-choline into d9-TMA, as described under Methods. For all plots, data reported are mean (\pm SEM) (middle bar and whiskers) for the indicated numbers of mice. The Wilcoxon rank-sum test was used for two-group comparison.

Figure 6. Over expression of human *fmo3* transgene in mice leads to increased platelet responsiveness and enhanced thrombosis potential *in vivo*. (A, B) Platelets rich plasma was isolated from human liver specific FMO3-TG mice and their WT littermates maintained on a choline (1%) supplemented diet. Plasma TMA and TMAO levels were quantified by stable isotope dilution LC/MS/MS analysis, and platelet aggregometry was monitored following stimulation with sub-maximal (1 μ M final) ADP, as described under Methods. (A) Representative aggregation tracings in response to ADP from a mouse within each group, along with plasma TMAO level in the mouse. (B) Cumulative data from mice in each group. Data represent the % of max aggregometry amplitude in response to 1 μ M ADP, along with mean (\pm SEM) plasma TMA and TMAO levels, for the indicated mouse groups. (C) Washed isolated platelets were recovered from hepatocyte-specific FMO3-TG mice and their WT littermates maintained on a chow (non-supplemented with choline) diet, and then surface expression of P-selectin in response to submaximal ADP (1 μ M) was determined by flow cytometry, as described in Methods. P-selectin surface expression (median fluorescence intensity, mean \pm SD) from the indicated number of mice are shown. (D, E) Vital microscopy images and quantified time to cessation of blood flow in carotid artery following FeCl₃-induced carotid artery injury in the indicated groups of mice. (E) Plasma TMA and TMAO levels are also shown. For all panels, the middle line represents mean and whiskers represent SEM for the indicated numbers of mice. The Wilcoxon rank-sum test was used for two-group comparison.

Figure 7. Microbial taxa associated with FMO3-TG-induced TMAO generation and a prothrombotic phenotype. (A) Correlation (spearman) between plasma TMAO levels and platelet aggregation response measured in human FMO3-TG mice and their WT littermates. (B-H) Cecal microbial composition was examined by 16S analyses in human FMO3-TG mice and their WT littermates following the carotid artery FeCl₃ injury model, as described under Methods. (B) Principal coordinates analyses demonstrate distinct cecal microbial composition between WT (blue) and

FMO3-TG (red) groups ($p < 0.001$ for Student's t test with 1,000 Monte Carlo simulations). Each data point represents a sample from a distinct mouse projected onto the first three principal coordinates (percent variation explained by each PCo is shown in parentheses). (C) Linear discriminant analysis (LDA) effect size (LEfSe) analyses were performed to identify taxa most characteristic (increased abundance) in WT (blue) and FMO3-TG (red). (D-G) Taxa whose proportions are significantly associated with both plasma TMAO levels and time to cessation of blood flow (occlusion time). P-Values shown are for comparison between different groups using a robust Hotelling T^2 test, with data expressed as mean (\pm SEM). (H) Correlation heat map showing taxa whose proportions are significantly associated with serum TMAO levels or vessel occlusion time. Red denotes a positive association, blue a negative association, and white no association. Single asterisk (*) indicates significant false discovery rate (FDR)-adjusted association of $p \leq 0.01$.

Figure 8. Summary scheme illustrating FMO3 involvement in TMAO generation, and enhanced thrombosis susceptibility. The host hepatic enzyme FMO3 plays a critical role in the metaorganismal TMAO generation pathway, linking dietary sources of choline abundant in a Western diet and gut microbiota-dependent generation of TMA with TMAO generation. Results from the present and other studies reveal TMAO plays a direct role in augmenting platelet responsiveness to multiple agonists, promoting arterial endothelial cell activation, and enhancing susceptibility for thrombosis. Multiple clinical studies show TMAO is dose dependently associated with adverse thrombotic event risk and mortality.

Figure 1

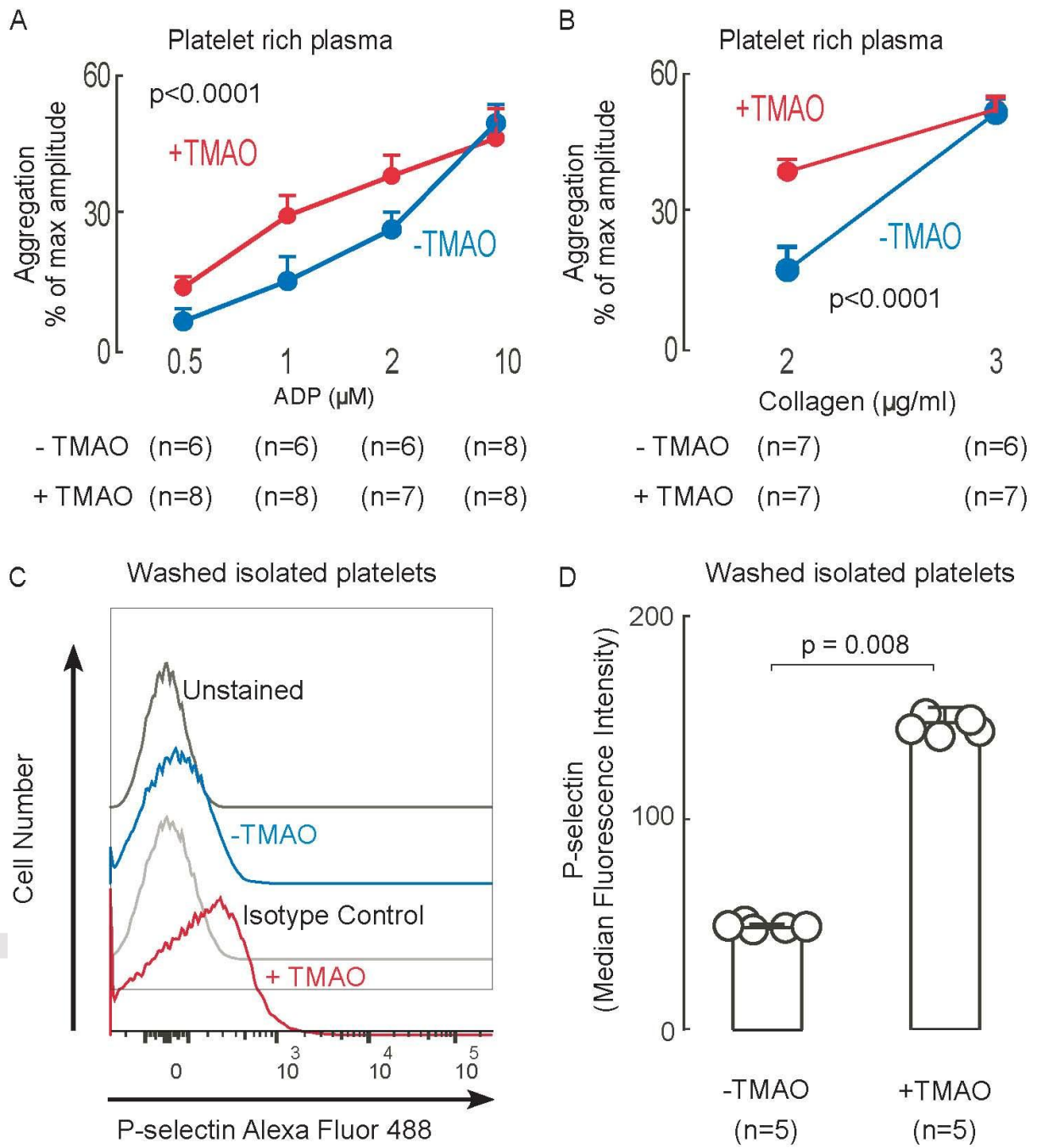


Figure 2

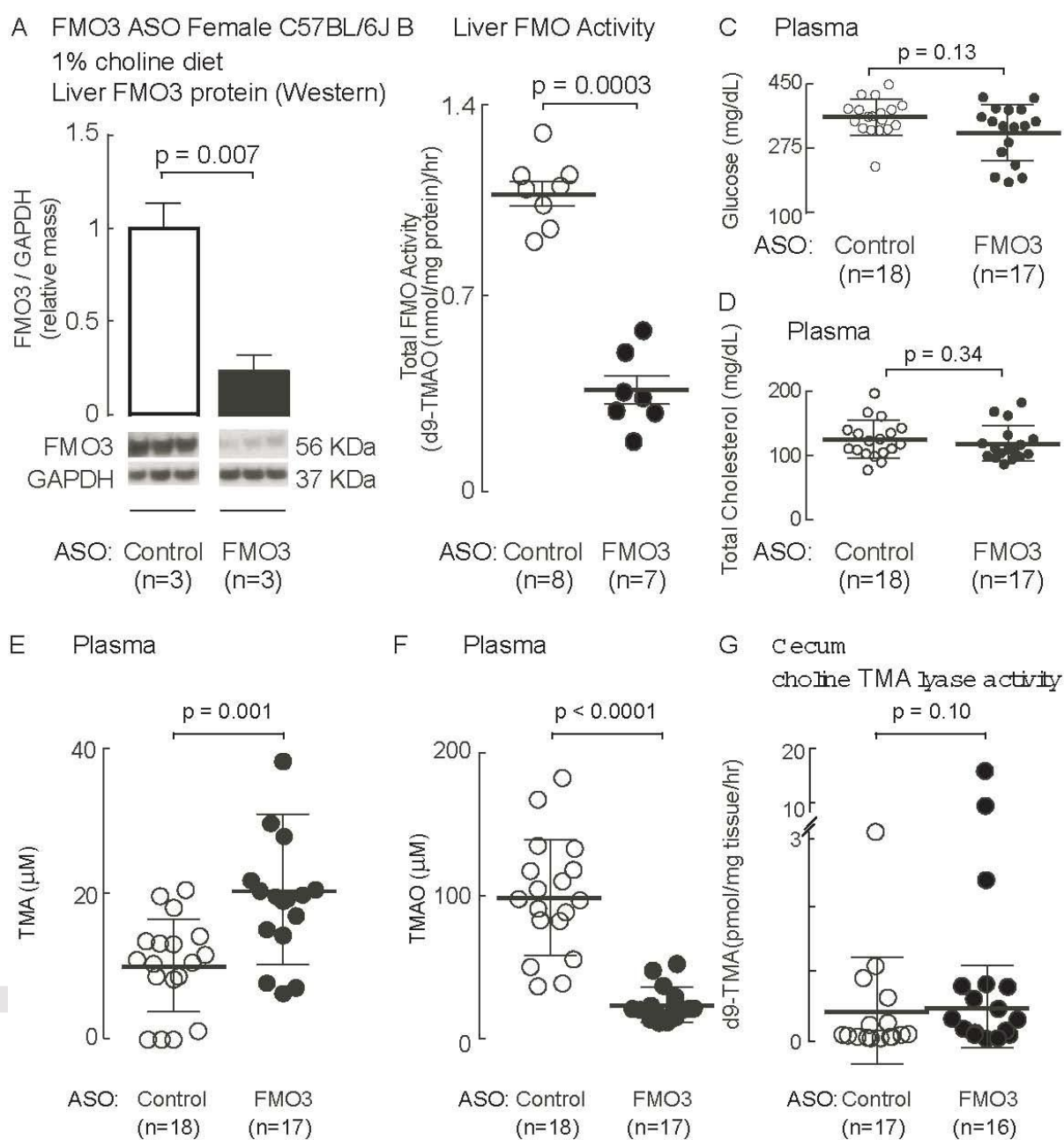


Figure 3

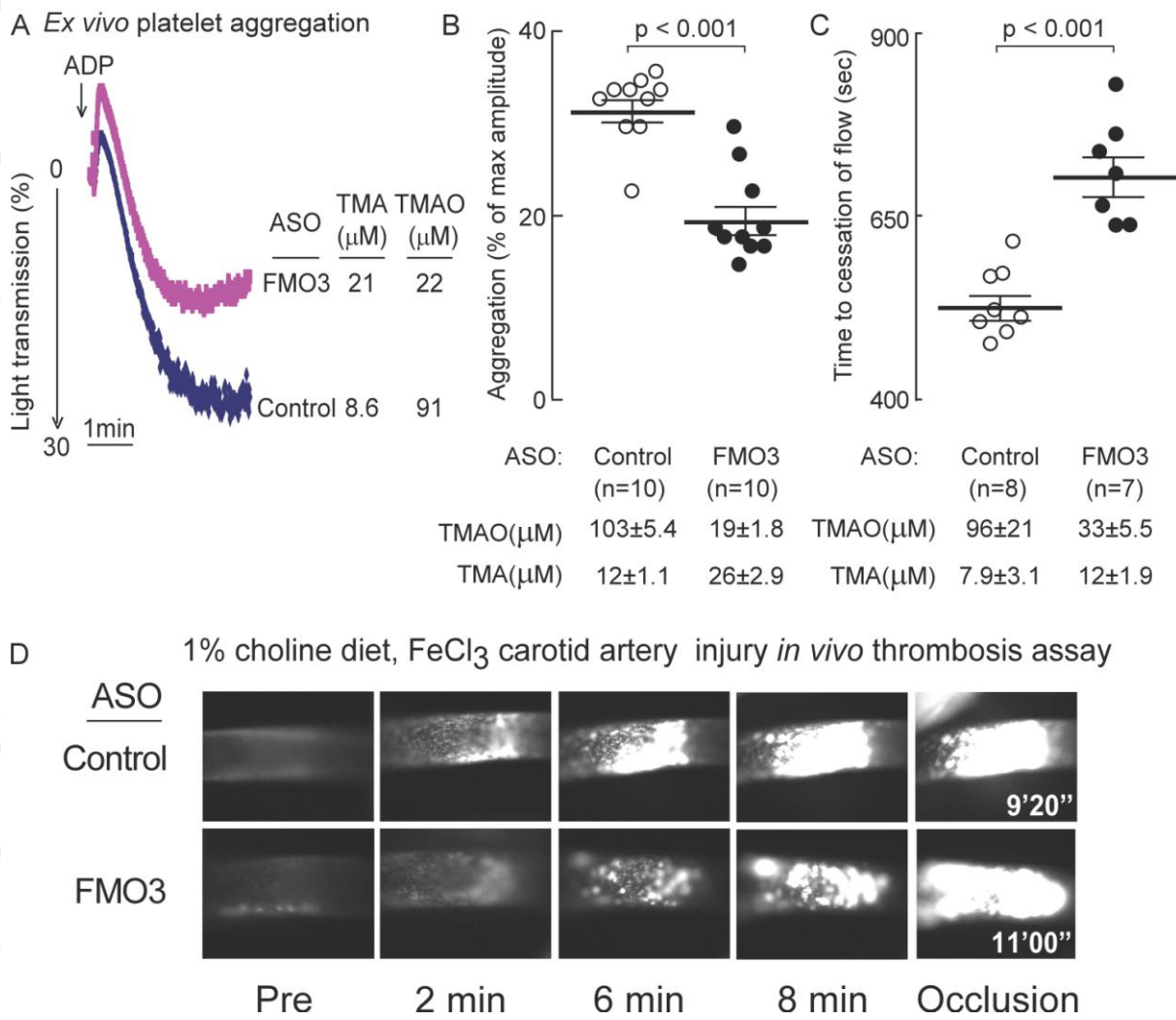
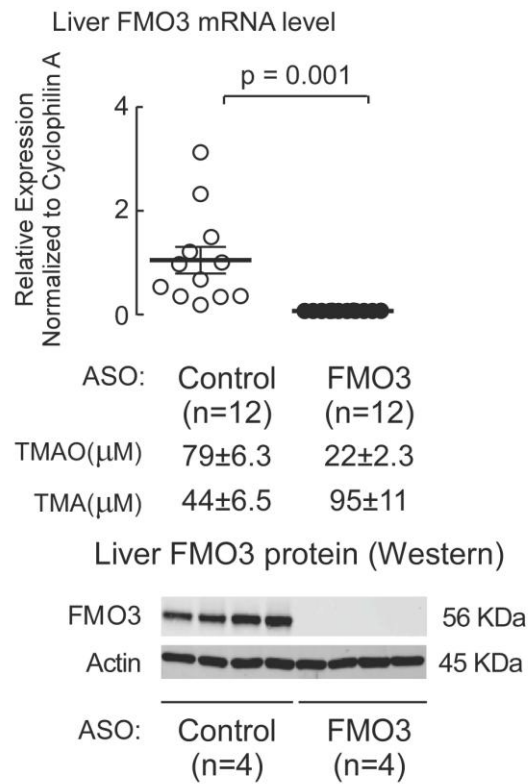
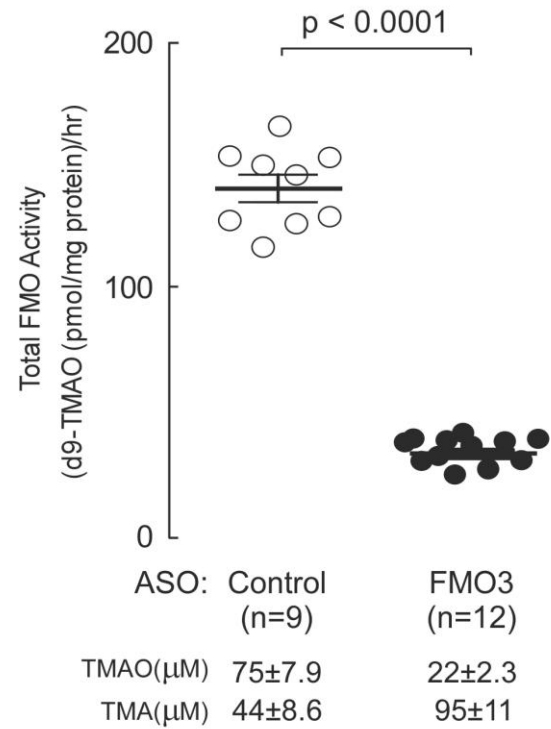


Figure 4

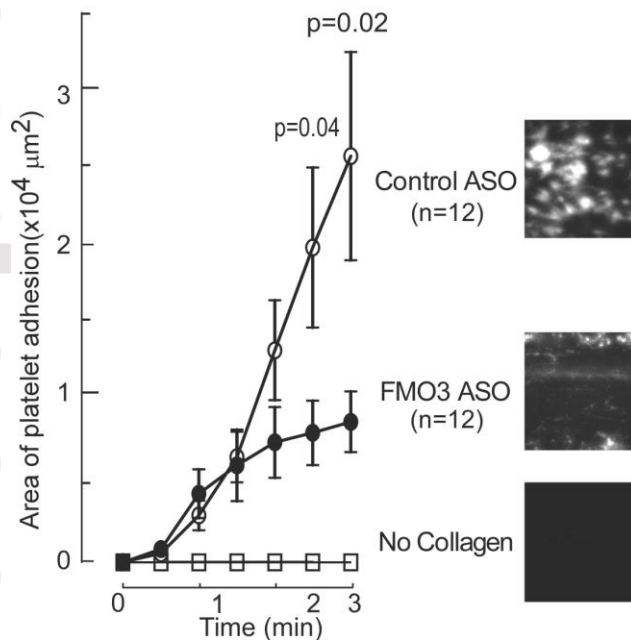
A FMO3 ASO Female C57BL/6J



B Liver FMO Activity



C Whole blood, microfluidic analysis



D TMAO(μ M)

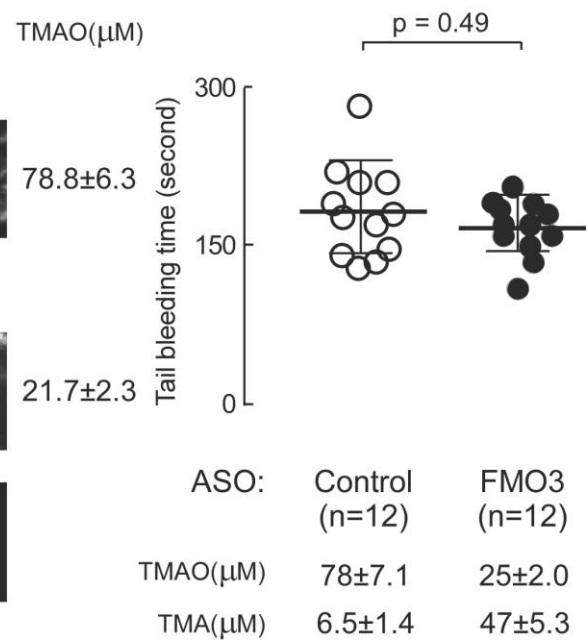


Figure 5

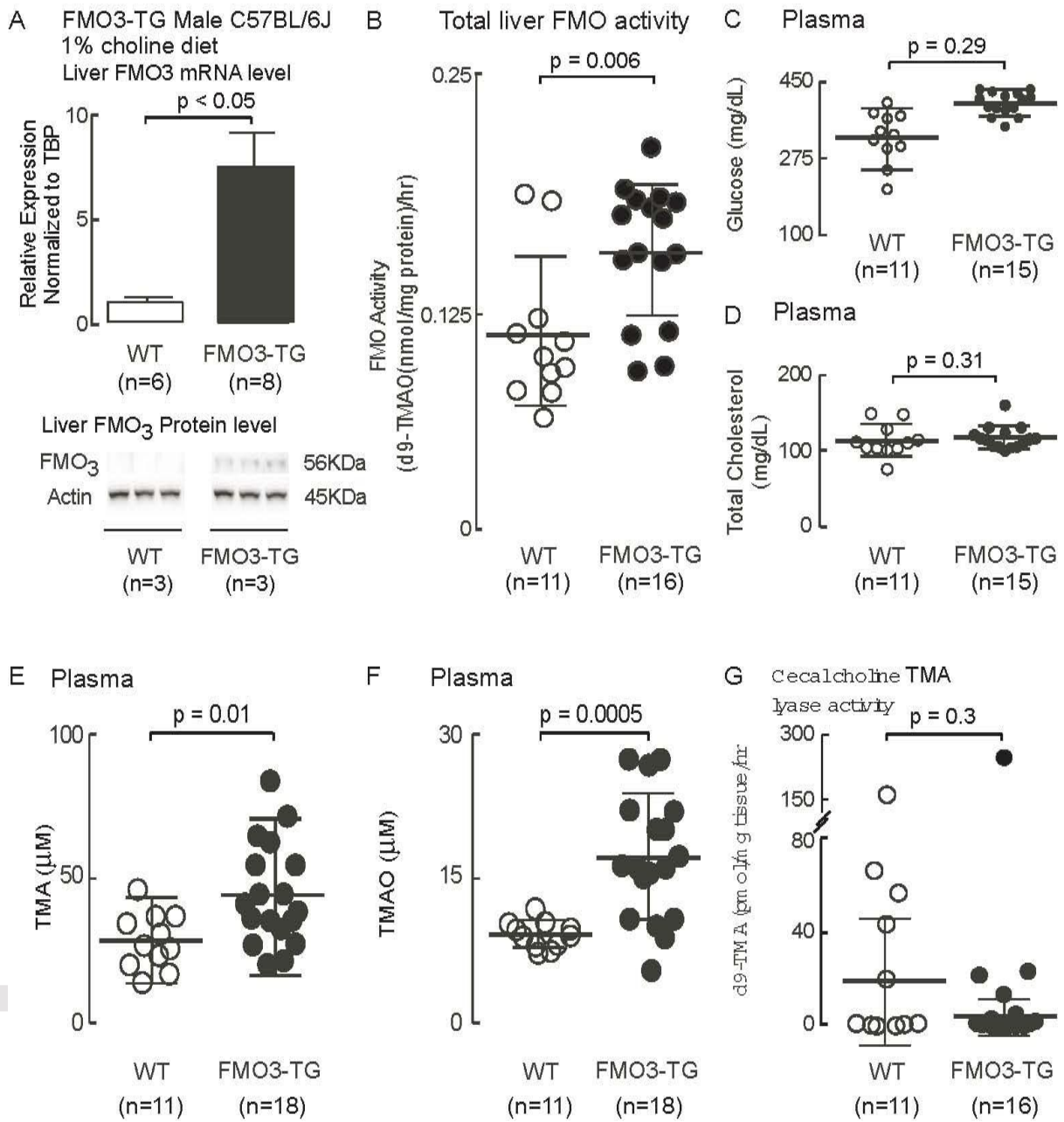


Figure 6

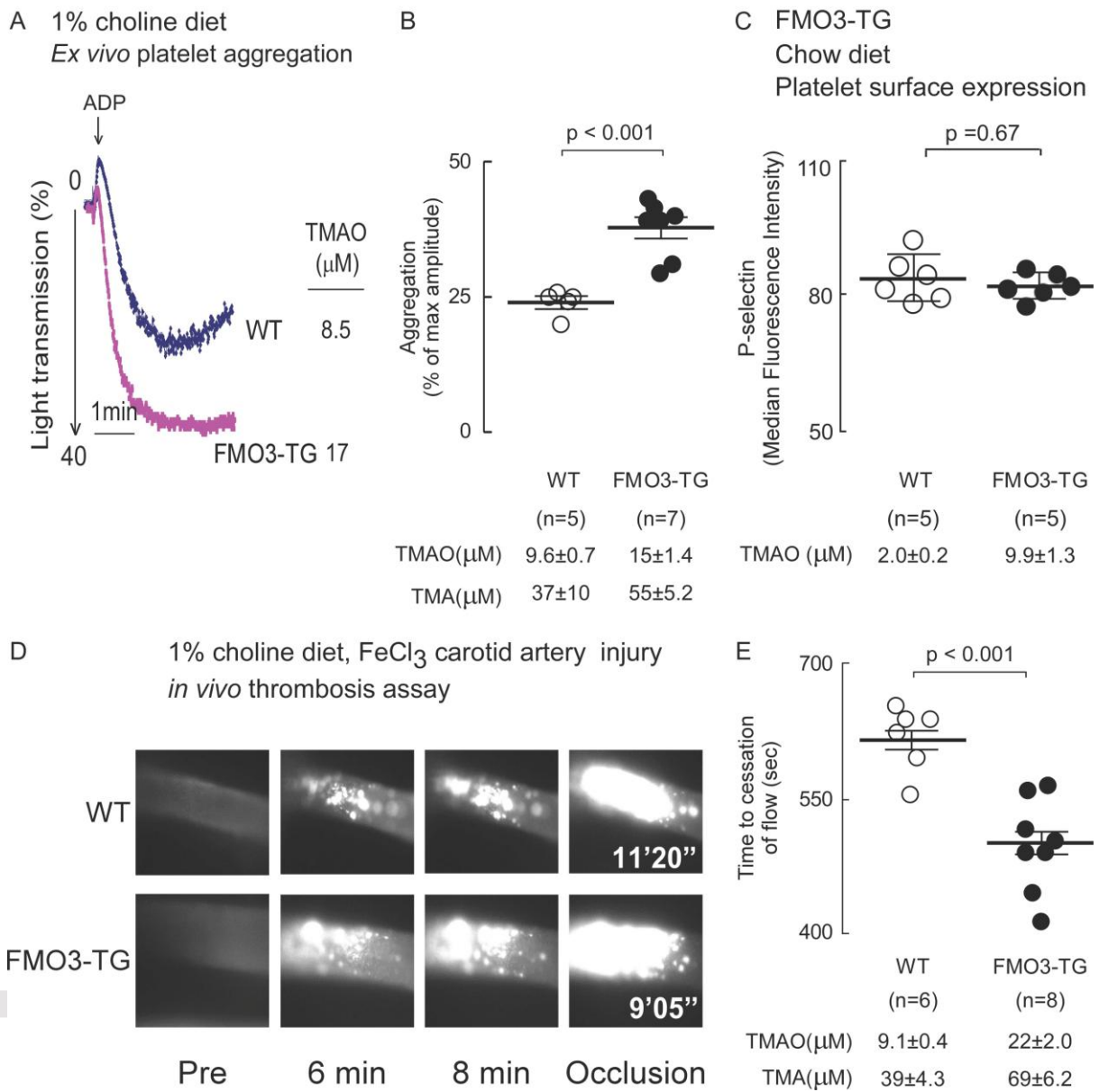


Figure 7

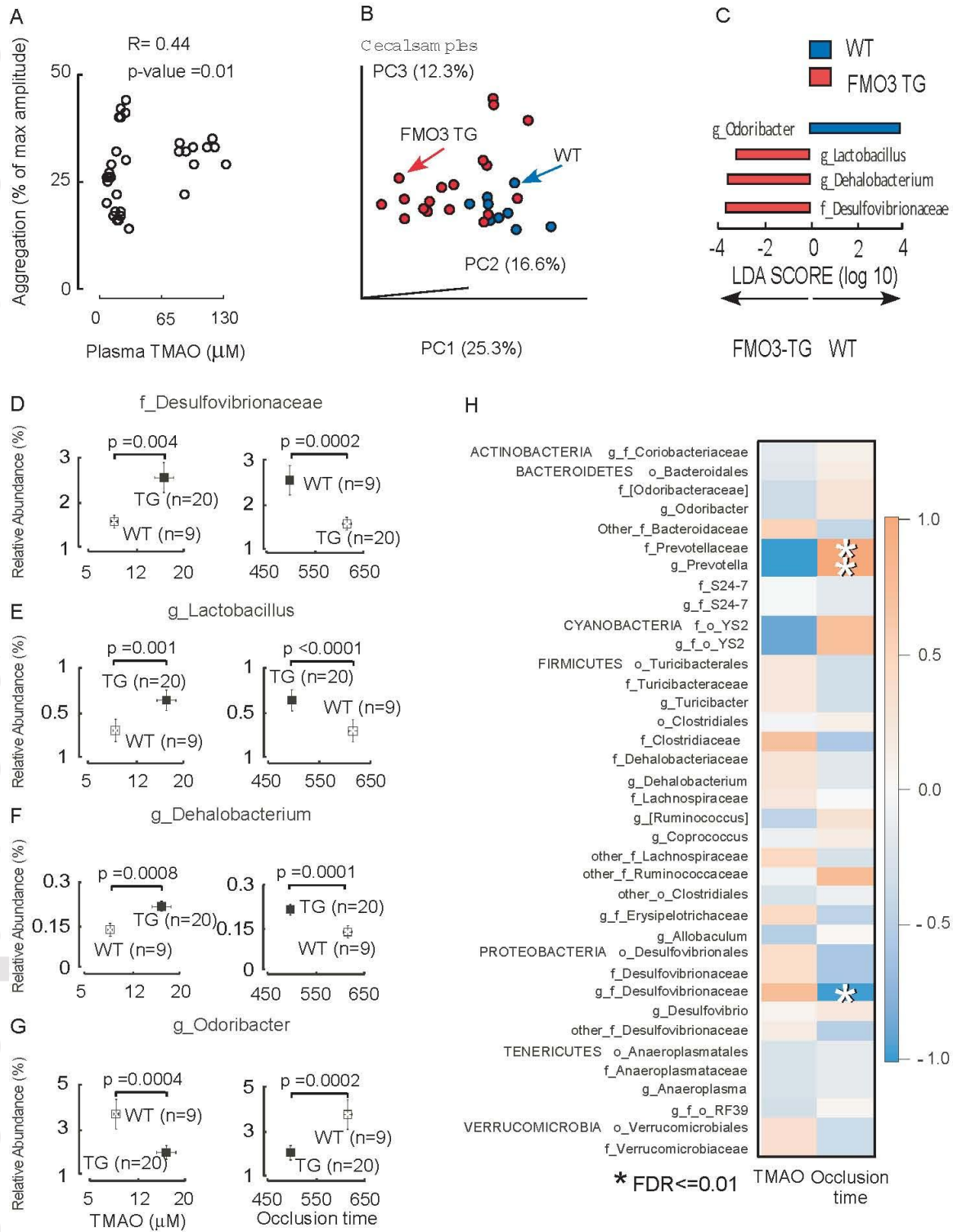


Figure 8

